

## **QUANTITATIVE PRETREATMENT $^{99m}\text{Tc}$ -MAA SPECT/CT AND FDG PET/CT VOI ANALYSIS OF LIVER METASTASES: RELATIONSHIP WITH TREATMENT RESPONSE TO SIRT**

Christophe Van de Wiele\*, M.D., Ph.D., Karin Stellamans, M.D.<sup>°</sup>, Eddy Brugman, M.D.<sup>°°</sup>,  
Gilles Mees\*, M.Sc., Bart De Spiegeleer\*\*, Ph.D., Yves D'Asseler\*, Ph.D., Alex Maes<sup>°°°</sup>,  
M.D., Ph.D.

\* Department of Nuclear Medicine, University Hospital Ghent, Belgium

° Department of Radiotherapy, AZ Groeninge, Kortrijk, Belgium

°° Department of Radiology, AZ Groeninge, Kortrijk, Belgium

\*\* Department of Analytical Chemistry, University Ghent, Belgium

°°° Departments of Nuclear Medicine, AZ Groeninge, Kortrijk, Belgium and Department  
of Morphology and Medical Imaging, University Hospital Leuven, Belgium

Address for correspondence and reprint requests : Christophe Van de Wiele, M.D., Ph.D.,  
Department of Nuclear Medicine, University Hospital Ghent, De Pintelaan 185B, 9000 Ghent,  
Belgium.

Tel: 0032/93323028, fax: 0032/93323807; e-mail: [christophe.vandewiele@ugent.be](mailto:christophe.vandewiele@ugent.be)

## **ABSTRACT**

**PURPOSE:** In this study, using quantitative VOI analysis, the percentage  $^{99m}\text{Tc}$ -MAA uptake and SUVmax and mean values of liver metastases obtained prior to SIRT by means of Theraspheres were related to treatment response.

**METHODS:** Pretreatment FDG PET/CT scans and  $^{99m}\text{Tc}$ -MAA SPECT/CT scans as well as post-treatment FDG PET/CT scans were coregistered and spherical VOI's drawn around FDG positive liver lesions on the pre-treatment scan using CT for contourdelineation. VOI's were then copied on the  $^{99m}\text{Tc}$ -MAA SPECT/CT scan and on post-treatment FDG PET/CT scans. VOI SUV mean and max values were obtained and the VOI counts derived from the  $^{99m}\text{Tc}$ -MAA SPECT/CT images divided by the total  $^{99m}\text{Tc}$ -MAA counts in the liver lobe or whole liver, depending on the procedure used, yielding the % of  $^{99m}\text{Tc}$ -MAA activity injected that ended up in the lesions. Based on the VOI % of  $^{99m}\text{Tc}$ -MAA activity, the estimated  $^{90}\text{Y}$ -Therasphere activity/cc (MBq/cc) was calculated from the effective dose of  $^{90}\text{Y}$ -Therasphere injected and by dividing with the VOI-volume in cc. Baseline VOI SUVmean and max values and estimated MBq/cc values were related to treatment response using a clinical dichotomous approach as well as a lesion based approach (% change in SUVmean  $\geq$  50 %).

**RESULTS:** Ninety-one lesions (18 therapeutic sessions in 16 patients) were analyzed; 57 responded and 34 did not (dichotomous approach). VOI volumes and estimated  $^{90}\text{Y}$ -Therasphere activity (MBq/cc) did not differ between responders and non responders; 24 cc (SD: 27) versus 21 cc (sd:21 cc) ( $p=0.4$ ) and (1.95 MBq/cc (SD: 1.1 MBq/cc) versus 1.90 MBq/cc (SD:2.7 MBq/cc) ( $p=0.92$ ). Also, activity in MBq/cc was not related to lesion size ( $p=0.32$ ). Contrariwise, SUVmax and mean values proved significantly different between responders and non-responders; 23.7 (SD 9.8) versus 9.4 (SD: 3.8 ) for SUVmax ( $p =0.0001$ ) and 13.1 (SD:8.1) versus 4.9(SD:1.4) for SUVmean. ROC curve analysis revealed an AUC for SUVmax and mean of respectively 0.87 and 0.81 ( $p=0.6$ ) for separating responders from

non-responders. Using the lesional approach and a cut-off of 50 % or more reduction in SUVmean for a responding lesion, 40 out of 77 lesions responded and 37 did not. SUVmax and mean values also proved significantly different between non-responding and responding lesions; 18.6 (SD 10.8) versus 13.5 (SD: 8.4 ) for SUVmax (p =0.02) and 11.4 (SD:3.8) versus 6.3(SD:4.5) for SUVmean (p=0.002). ROC curve analysis revealed and AUC for SUVmax and SUVmean for separating responding from non-responding lesions of 0.7 and 0.65 (p= 0.6).

**CONCLUSION:** Baseline FDG SUVmax and mean values of non-responders/non-responding liver metastases to SIRT are significantly higher when compared to responders/responding lesions for a comparable estimated <sup>90</sup>Y-Therasphere activity/cc. Thus, in patients presenting with high baseline SUVmax and mean values, the administration of higher activities or alternatively, other potentially more useful treatment options might be considered.

*Key words: SIRT-VOI analysis- treatment response*

## INTRODUCTION

Selective internal radiation therapy (SIRT) or transarterial radioembolization using  $^{90}\text{Y}$ -labelled microspheres involves the intra-arterial injection of commercially available  $^{90}\text{Y}$ -labelled microspheres via the hepatic artery or a side-branch thereof [1-4]. As liver metastases are primarily fed via the hepatic artery, following their injection,  $^{90}\text{Y}$ -labelled microspheres will become entrapped in the tumor vasculature ;  $^{90}\text{Y}$ -labelled microspheres are small enough to pass deep into the tumor vasculature but too large to pass through the capillary bed and reach the venous circulation. Following entrapment in the tumor vasculature,  $^{90}\text{Y}$  will decay (half-life: days), emitting  $\alpha$ -particles with an average energy of 0.9367 Mev and a mean tissue penetration of 2.5 mm (maximum penetration = 1 cm). As such SIRT is a form of low-dose rate intra-arterial brachytherapy. As with other forms of brachytherapy, the presence of oxygen is a prerequisite for fixing the damaging effects induced by the  $\alpha$ -radiation via free radical reaction mechanisms in SIRT. Accordingly, when confronted with structural hypoxia due to inadequate vascularization, a poor response to SIRT may be anticipated.

In order to confirm access to areas of the liver that need to be treated with  $^{90}\text{Y}$ -labelled microspheres and in order to isolate liver from other foregut structures, prior to selective internal radiation therapy (SIRT) of livermetastases, a  $^{99\text{m}}\text{Tc}$ -MAA scan is performed. As  $^{99\text{m}}\text{Tc}$ -MAA is assumed to have a similar particle size to that of  $^{90}\text{Y}$ -labelled microspheres the biodistribution of  $^{99\text{m}}\text{Tc}$ -MAA particles within the liver is also assumed to be similar to that of  $^{90}\text{Y}$ -labelled microspheres and to reflect tumor arterial vascularization relative to normal tissue [5,6]. Accordingly, liver lesions with high  $^{99\text{m}}\text{Tc}$ -MAA uptake can be expected to receive a high dose of  $^{90}\text{Y}$ -labelled microspheres. Inversely, in poorly vascularized liver

lesions as reflected by a low uptake of  $^{99m}\text{Tc}$ -MAA a poor response to treatment may be anticipated.

In this study, using quantitative VOI analysis, flow as assessed by  $^{99m}\text{Tc}$ -MAA imaging and metabolism as assessed by FDG PET imaging of liver metastases prior to SIRT was studied and findings obtained related to treatment outcome.

## **PATIENTS AND METHODS**

In all patients under study, a baseline FDG PET scan was performed within 4 weeks of the  $^{99m}\text{Tc}$ -MAA scan as part of a routine work-up on a dedicated BGO PET system with a helical CT (Discovery LS; GE Healthcare). Images were acquired 60 minutes following the injection of  $x$  MBq FDG, depending on the body mass index of the patient.

Therasphere treatment was performed as described previously by Salem et al. First an angiography was performed for the purpose of coiling collateral gastrointestinal vessels. Subsequently, in order to confirm access to areas of the liver that need to be treated with  $^{90}\text{Y}$ -labelled microspheres and in order to isolate liver from other foregut structures as well as to assess the degree of lungshunting, at the end of the first angiography a  $^{99m}\text{Tc}$ -MAA scan was performed following the injection of 111 MBq freshly prepared  $^{99m}\text{Tc}$ -labelled MAA. Both a whole body scintigraphy (15 minutes) and a SPECT-CT scan were obtained (step and shoot modus; matrixsize 128x128) using a dual-headed GE SPECT-CT camera equipped with LEHR collimators (Infinia, GE Medical Systems, Milwaukee, WI, USA). Images were reconstructed using an ordered subset expectation maximization software programme provided by the vendor. In none of the patients included extrahepatic activity occurred on the  $^{99m}\text{Tc}$ -MAA scan other than in the lungs (estimated dose inferior to 30 Gy, see below): percentage lung shunting was  $\leq 3\%$  in all patients studied. One to two weeks later,

Theraspheres were injected during a second angiography targeting a dose of  $120 \pm 20$  Gy to the target volume whilst not exceeding a dose of 30 Gy to the lungs. The dose was calculated as described previously by Salem et al. The volume of the treated liver lobe was considered as target volume and measured on CT. Injection of Theraspheres was performed manually using the plexiglass-shielded injection system provided by the vendor (Nordion, France). On the day of treatment a post-treatment brehmsstrahlung whole body scan and a SPECT-CT of the liver was performed to confirm the localization of the  $^{90}\text{Y}$ -microspheres in the liver. Patients were allowed to leave the hospital the day after the therapeutic injection. Response to treatment of liver lesions was assessed between 4-5 weeks following treatment based on changes on contrast-enhanced CT findings (available in all patients) and on sequential FDG PET/CT imaging (available in 14 treatment sessions) as well as on changes in serum marker measurements, when available. In case the patient was deemed a responder, all lesions were categorized as responding and vice-versa for non-responders. Aside from this clinical dichotomous approach, when a follow-up PET-CT examination was available, a lesion based analysis was also performed using a cut-off of  $< 50\%$  in SUVmax and SUVmean to separate non-responding from responding lesions.

## **IMAGE PROCESSING AND DATA ANALYSIS**

### **Image coregistration**

The baseline FDG PET/CT scan and the  $^{99\text{m}}\text{Tc}$ -MAA SPECT/CT scan were co-registered using the baseline FDG PET/CT scan as template using PMOD software (PMOD Technologies Ltd.; Zurich, Switzerland). Following image co-registration, images were resliced to the voxelsize of the PET images.

## **Lesion delineation and data comparison**

Given the patients in this study were all multi-treated, CT was not used for selection of relevant lesions given its unreliability due to the presence of necrosis or cystic changes. Instead, relevant lesions were identified on the FDG PET images. Around isolated FDG PET positive liver lesions a spherical VOI was drawn that encompassed the lesion as defined on the corresponding CT images; minimal diameter of lesions included was 2 cm. From the VOIs drawn, the SUVmax and SUVmean values of the lesions were derived. VOIs obtained were subsequently copied on the corresponding  $^{99m}\text{Tc}$ -MAA scan.  $^{99m}\text{Tc}$ -MAA was injected either in the right or left liver lobe or in the common hepatic artery, depending on the planned treatment. Separate counts in  $^{99m}\text{Tc}$ -MAA VOIs and SUV's in FDG PET VOIs were obtained and divided by the total  $^{99m}\text{Tc}$ -MAA activity in the liver, yielding the % of the dose of  $^{99m}\text{Tc}$ -MAA injected that ended up in the lesion as defined by the VOI encompassing it. Thus obtained percentages were subsequently used to derive the  $^{90}\text{Y}$ -Therasphere activity deposited based on the actual dose of  $^{90}\text{Y}$ -Theraspheres injected, which was subsequently divided by the VOI volume in cc, yielding the trapped estimated activity of  $^{90}\text{Y}$ -Theraspheres in MBq/cc. While the percentage lung shunting was  $\leq 3\%$  in all patients studied, it was deemed to be 0% for analysis.

When available, VOI's were also copied on the post-therapy FDG PET/CT examination, available in 14 sessions, obtained between 4-5 weeks after treatment. For comparison with available literature in the field, SUV mean values were also derived from the post-treatment FDG PET/CT scan (following image fusion using the baseline examination as reference and following copying of the VOIs drawn on the baseline) and the percentage reduction in SUVmean calculated [7]. Subsequently, two groups of lesions were defined, respectively

responding and non-responding lesions using a cut-off value of  $\geq 50\%$  reduction for responding lesions.

## **STATISTICAL ANALYSIS**

Statistical analysis was performed using SPSS version 20.0. Normalcy of data was assessed using the Kolmogorov-Smirnov test. Correlation analysis was performed using Pearson-correlation analysis. An unpaired student t-test was used for assessing differences between responding and non-responding lesions in SUV max and mean values as well as in trapped  $^{90}\text{Y}$ -Therasphere activity. ROC curve analysis was also performed.

## **RESULTS**

Thirteen patients suffering from liver metastases, corresponding to 15 treatment sessions, were included in the study (5 men/9 women; age range : 56-79 years). With the exception of two patients who underwent a whole liver treatment (single treatment), treatments were performed on a lobar base. Nine patients underwent a single, unilobar treatment, in eight patients the right liver lobe was treated and in one patient the left lobe was treated. Two patients underwent a separate treatment of their right and left liver lobe. Overall, there were 15 therapeutic sessions : dose range administered was 0.75 -7.17 GBq (mean : 3.5 GBq).

### ***Lesion based analysis using a dichotomous clinical approach (responder versus non-responder):***

Overall, ninety-one lesions were analyzed, of which 57 responded and 34 did not respond to treatment (responder versus non-responder). The mean volume of lesions included was 23 cc



(sd: 26 cc, range 4-155 cc). Mean activity in MBq/cc of  $^{90}\text{Y}$ -Theraspheres of all lesions analyzed was 1.9 MBq/cc (sd : 1.9, range : 0.2-12.9). Mean SUVmax and SUV mean values of all lesions analyzed were respectively 14.2 (sd: 9.6, range : 3.6-38.1) and 7.7 (sd: 6.3, range : 2.3-26.7). Activity in MBq/cc was not related to lesion size ( $p= 0.32$ , see Figure 1). SUVmax and SUV mean of lesions were not significantly correlated with the activity in MBq/cc of  $^{90}\text{Y}$ -Theraspheres ( $p = 0.159$  and  $p = 0.141$ ).

Mean lesional volume proved not significantly different between responding and non-responding lesions (24cc (sd: 27 cc, range 4-155cc) versus 21 cc (sd : 21 cc, range : 4-113cc), ( $p = 0.4$ ). Activity in MBq/cc of  $^{90}\text{Y}$ -Theraspheres proved not significantly different between responding and non-responding lesions; 1.95 MBq/cc (sd 1.1 MBq/cc) in non - responding lesions versus 1.90 MBq/cc (sd: 2.7 MBq/cc) in responding lesions ( $p = 0.92$ ).

Mean SUV max and mean values proved significantly different between non-responding and responding lesions; 23.7 (sd: 9.8, range : 4.4-38) for SUV max and 13.1 (sd: 8.1, range : 2.6-26.7) for SUV mean in non - responding lesions versus 9.4 (sd: 3.8, range : 4-20.1) for SUV max and 4.9 (sd: 1.4, range : 2.3-8.6) SUV mean in responding lesions ( $p = 0.0001$ ). ROC curve analysis revealed an AUC for SUV max and SUV mean for separating responders from non-responders of 0.87 and 0.81 respectively ( $p = 0.6$ ). Using a cut-off of 16.3 for SUV max, responding lesions could be separated from non-responding lesions with a sensitivity of 85 % and a specificity of 95%. See figure 2. Using the average SUV max values of all lesions per patient as representative for all liver lesions, ROC curve analysis yielded the same AUC value and the cut-off value of 16.3 the same sensitivity and specificity.

***Lesion-based response analysis using a cut-off of < 50% reduction in SUVmean and SUVmax (follow-up PET):***

Using a cut-off of 50% or more reduction in mean SUV for a responding lesions, of 77 evaluable lesions, 40 lesions were shown to respond and 37 not. On a lesional basis, mean lesional volume proved not significantly different between responding and non-responding lesions (22cc (sd: 27 cc) versus 23 cc (sd : 23 cc ), ( p = 0.69). Activity in MBq/cc of <sup>90</sup>Y-Theraspheres proved not significantly different between responding and non-responding lesions; 1.7 MBq/cc (sd 1.8 MBq/cc) in non - responding lesions versus 2.1 MBq/cc (sd: 2.1 MBq/cc) in responding lesions (p = 0.47).

Mean SUV max and mean values proved significantly different between non-responding and responding lesions; 18.6 (sd: 10.8, range : 4.6-38.1) for SUV max and 11.4 (sd: 3.8, range : 3.2-26.7) for SUV mean in non - responding lesions versus 13.5 (sd: 8.4, range : 3.6-33.3) for SUV max and 6.3 (sd: 4.5, range : 2.3-21.7) SUV mean in responding lesions (p = 0.02 and p =0.002). ROC curve analysis revealed an AUC for SUV max and SUV mean to separate responding from non-responding lesions of 0.7 and 0.65 respectively ( p = 0.6).

## **DISCUSSION**

<sup>99m</sup>Tc-MAA scintigraphy allows assessment of the magnitude of the flux of blood into and of the vascular spaces able to accommodate the radioactive microspheres and their eventual outlets that allow particles to escape in both tumorous and non-tumorous liver tissue. As the particle size of <sup>99m</sup>Tc-MAA is deemed to be similar to that of Theraspheres, liver lesions with high <sup>99m</sup>Tc-MAA uptake may be expected to receive a high dose of <sup>90</sup>Y-Theraspheres and thus respond better than tumors demonstrating a low uptake. A limited number of studies have reported on the predictive value of <sup>99m</sup>Tc-MAA imaging for treatment response in SIRT. Dhabuwala et al. retrospectively reviewed pretreatment <sup>99m</sup>Tc-MAA planar scans of 58 patients with colorectal hepatic metastases that were treated by SIRT. Tumors were

qualitatively considered cold, equivocal or hot based on  $^{99m}\text{Tc}$ -MAA uptake and the ratio of uptake in tumor and normal tissue [8]. Data obtained were related to treatment response performed using RECIST criteria and changes in serum markers. CT responses and drops in CEA level after three months proved similar between patients presenting with “hot” metastases and patients presenting with “equivocal and cold” metastases on  $^{99m}\text{Tc}$ -MAA scans. Flamen et al. mathematically converted liver voxel  $^{99m}\text{Tc}$ -MAA-SPECT values to the absolute  $^{90}\text{Y}$ -SIRspheres activity on images obtained in 8 evaluable patients that underwent SIRT. Subsequently the absolute  $^{90}\text{Y}$ -SIRspheres activity per voxel was then converted to a simulated absorbed dose using an S-factor for the liver for  $^{90}\text{Y}$  of 18.1 mGy/MBq (residence time = 2.67 days) [7]. VOIs encompassing liver metastases, 39 in total, were then defined on a pretherapy FDG PET examination using segmentation and copied on the  $^{99m}\text{Tc}$ -MAA scans allowing calculation of the mean simulated absorbed dose value for all voxels within the lesion. Additionally, tumor-to-background ratio's were determined on the  $^{99m}\text{Tc}$ -MAA images for all lesions. Using post-therapy FDG PET imaging for response assessment and a cut-off of 50 % reduction in total lesion glycolysis of studied lesions, an area under the curve of 0.86 was found on ROC-analysis for the mean simulated absorbed dose, corresponding linearly to the average activity within each VOI of  $^{99m}\text{Tc}$ -MAA, for separating responding from non-responding lesions. In the series presented, using a lesion-based approach as well as a patient-based approach, no difference in activity in MBq/cc of  $^{90}\text{Y}$ -Theraspheres and consequently also in  $^{99m}\text{Tc}$ -MAA activity or counts was found between responders and non-responders. These findings are, however, not in contradiction with the series by Flamen et al. First, while in the series by Flamen et al. non-responding lesions and responding lesions had similar mean SUVmean values, respectively 6.1, in our series, mean SUVmax and SUVmean values of non-responding lesions were significantly higher when compared to non responding lesions (18.6 and 11.4 versus 13.5 and 6.3; lesional analysis). Second, whereas the average simulated

activity contained by non-responding lesions was  $488\pm 392$  kBq/ml versus  $1329\pm 1.219$  kBq/ml for responding lesions by Flamen et al., in the series presented, non-responding lesions (lesional approach) contained an average activity of  $2100\pm 2100$  kBq/ml. This activity, which was comparable to the average activity contained by responding lesions in this series, is well above the dose received by the responding lesions in the series by Flamen et al. The difference in simulated activity contained by lesions between both series is not that surprising given the maximum administrable dose for SIRspheres is 3 GBq, regardless of the to be treated liver volume, versus 20 GBq for Theraspheres, on the one hand and the currently adopted whole liver approach for SIRspheres versus unilobar approach for Theraspheres on the other hand. Hypothetically, the lower activity contained by lesions in the series by Flamen et al. might be volume-related; the lesions included for analysis in the series by Flamen et al. were significantly larger when compared to this series ( respectively  $160\pm 266$  cc versus  $23\pm 6$  cc). However, within the range of volumes studied in this study, the average activity per volume unit proved unrelated to the lesion volume (see Figure 1).

Of interest, both the lesional as well as clinical strategy to separate responding lesions from non-responding lesions put to evidence a significant difference in SUVmax and SUVmean values between both; non responding lesions had a significantly higher FDG uptake when compared to responding lesions, while the simulated activity and size-distribution of lesions proved identical. From a biological point of view, this may be interpreted as a form of advanced adaptation of the tumor to the local environmental conditions, e.g. metabolism uncoupling of flow, beyond that secondary to oncogene effects alone resulting in an increase in tumor aggression and resistance to treatment [9-17]. In this regard, Haug et al. recently reported on a significantly shorter survival of patients suffering from liver metastases of a primary breast carcinoma presenting with baseline SUVmax values of liver metastases above 20, treated by SIRT [18]. Using a cut-off value of 16 for SUVmax, in our series, responding

lesions as well as responders (averaged values of all lesions per patient) could be separated from non-responders with a sensitivity of 85% and a specificity of 95% . Accordingly, in patients presenting with liver metastases with SUVmax values exceeding 16, the injection of higher-activities of  $^{90}\text{Y}$ -labelled microspheres might be considered, provided the thresholds for normal liver and lungs are not exceeded. A similar suggestion was recently also proposed by Garin et al. for the treatment of HCC using Theraspheres [19]. Alternatively, other potentially useful treatment options may be considered.

To conclude, in this study, the accumulated percentage activity of  $^{99\text{m}}\text{Tc}$ -MAA and thus of dose delivered when performing SIRT using Theraspheres for the treatment of liver metastases proved comparable between responding and non-responding lesions. Contrariwise, FDG PET SUVmax values of liver metastases on pretreatment FDG PET scans obtained in patients scheduled for treatment of livermetastases by means of SIRT proved significantly higher in non-responders. Accordingly, above a certain threshold of SUV max , e.g. 16 as derived in this series, the administration of higher activities of  $^{90}\text{Y}$ -labelled microspheres or alternatively, other potentially more useful treatment options might be considered. Additional studies in larger patient populations confirming these findings are warranted.

## REFERENCES

1. Van de Wiele C, Defreyne L, Peeters M, Lambert B. Yttrium-90 labelled resin microspheres for treatment of primary and secondary malignant liver tumors. *Q J Nucl Med Mol Imaging* 2009; 53: 317-324.
2. Garin E, Rolland Y, Boucher E, Ardisson V, Laffont S, Boudjema K, Bourguet P, Raoul JL. First experience of hepatic radioembolization using microspheres labelled with yttrium-90 (Therasphere): practical aspects concerning its implementation. *Eur J Nucl Med Mol Imaging* 2010; 37: 453-461.
3. Welsh JS, Kennedy AS, Thomadsen B. Selective internal radiation therapy (SIRT) for liver metastases secondary to colorectal adenocarcinoma. *JRBOP* 2006; 66: S62-S73.
4. Wong CY, Savin M, Sherpa KM, Qing F, Campbell J, Gates VL, Lewandowski RJ, Cheng V, Thie J, Fink-Bennett D, Nagle C, Salem R. Regional yttrium-90 microsphere treatment of surgically unresectable and chemotherapy refractory metastatic liver carcinoma. *Cancer Biother Radiopharm* 2006; 21: 305-313.
5. Salem R, Lewandowski RJ, Sato KT, Atassi B, Ryu RK, Ibrahim S, Nemcek AA Jr, Omary RA, MAdoff DC, Murthy R. Technical aspects of radioembolization with 90Y microspheres. *Tech Vasc Interv Radiol* 2007; 10: 12-29.
6. Lewandowski RJ, sato KT, Atassi B, Ryu RK, Nemcek AA Jr, Kulik L, Geschwind JF, Murthy R, Rilling W, Liu D, Bester L, Bilbao JI, Kennedy AS, Omary RA, Salem R. Radioembolization with 90Y microspheres: angiographic and technical considerations. *Cardiovasc Intervent Radiol* 2007; 30:571-592.
7. Flamen P, Vanderlinden B, Delatte P, Ghanem G, Ameye L, Van Den Eynde M, Hendlisz A. Multimodality imaging can predict the metabolic response of unresectable colorectal liver

metastases to radioembolization therapy with Yttrium-90 labelled resin microspheres. *Phys Med Biol* 2008; 53: 6591-6603.

8.Dhabuwala A, Lamerton P, Stubbs RS. Relationship of <sup>99m</sup>Tc-labelled macroaggregated albumin (<sup>99m</sup>Tc-MAA) uptake by colorectal liver metastases to response following selective internal radiation therapy (SIRT). *BMC Nuclear medicine* 2005; 5: 1-10.

9.Miles KA, Williams RE. Warburg revisited: imaging tumour blood flow and metabolism. *Cancer Imaging* 2008; 8: 81-86.

10.Fukuda K, Taniguchi H, Hoh T, Kunsihima S, Yamagashi H. Relationship between oxygen and glucose metabolism in human liver tumours: positron emission tomography using <sup>15</sup>O and <sup>18</sup>F-deoxyglucose. *Nucl Med Commun* 2004; 25: 577-583.

11.Stewart EE, Chen X, Hadway J, Lee TY. Correlation between hepatic tumor blood flow and glucose utilization in a rabbit liver tumor model. *Radiology* 2006; 239: 740-750.

12. Miles KA, Williams RE, Yu D, Griffiths MR. Demonstrating intertumoural differences in vascular-metabolic phenotype with dynamic contrast-enhanced CT-PET. *Int J Molecular Imaging* 2011; 2011: 1-8.

13.Aronen HJ, Pardo FS, Kennedy DN, et al. High microvascular blood volume is associated with high glucose uptake and tumor angiogenesis in human gliomas. *Clin Cancer Res* 2000; 6: 2189-2200.

14.Mankoff DA, Dunnwald LK, Gralow Jr et al. Blood flow and metabolism in locally advanced breast cancer: relationship to response to therapy. *J Nucl Med* 2002; 43: 500-509.

15.Miles KA, Griffiths MR, Keith CJ. Blood flow-metabolic relationships are dependent on tumour size in non-small cell lung cancer: a study using quantitative contrast-enhanced

computer tomography and positron emission tomography. *Eur J Nucl Med Mol Imaging* 2006; 33: 22-28.

16. Hermans R, Meijerink M, van den Bogaert W, Rijnders A, Weltens C, Lambin P. Tumor perfusion rate determined non-invasively by dynamic computed tomography predicts outcome in head-and-neck cancer after radiotherapy. *Int J Radiat Oncol Biol Phys* 2003; 57: 1351-1356.

17. Allal AS, Slosman DO, Kebdani T, Allaoua M, Lehmann W, Dulguerov P. Prediction of outcome in head-and-neck cancer patients using the standardized uptake value of 2-[<sup>18</sup>F]fluoro-2-deoxy-D-glucose. *Int J Radiat Biol Oncol Biol Phys* 2004; 5: 1295-1300.

18. Haug AR, Beauclair P, Donfack T, Trumm C, Zech CJ, Michl M, Laubender RP, Uebleis C, Bartenstein P, Heinemann V, Hacker M. <sup>18</sup>F-FDG PET/CT predicts survival after radioembolization of hepatic metastases from breast cancer. *J Nucl Med* 2012; 53: 371-377.

19. Garin E, Lenoir L, Rolland Y, Edeline J, Mesbah H, Laffont S, Porée P, Clément B, Raoul J-L, Boucher E. Dosimetry based on <sup>99m</sup>Tc-macroaggregated albumin SPECT/CT accurately predicts tumor response and survival in hepatocellular carcinoma patients treated with <sup>90</sup>Y-loaded glass microspheres: preliminary results. *J Nucl Med* 2012; 53: 255-263.



**FIGURES**

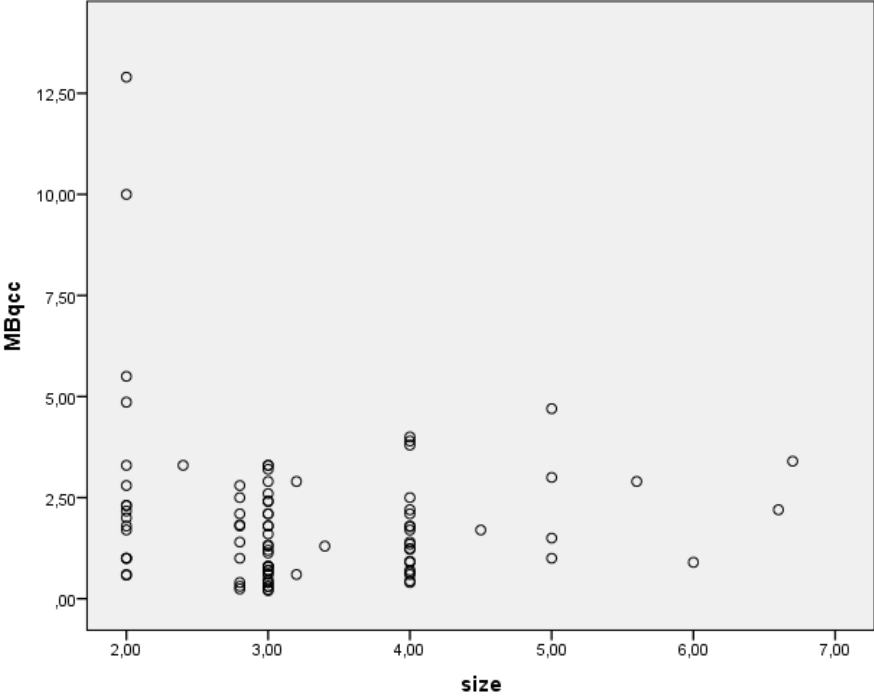


Figure 1 shows the relationship between lesion size (diameter derived from the VOI volume) and activity in MBq/cc

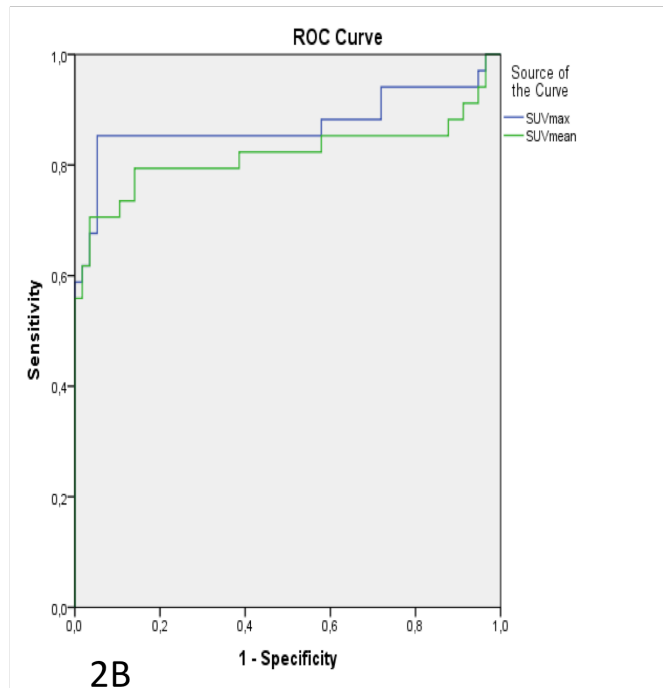
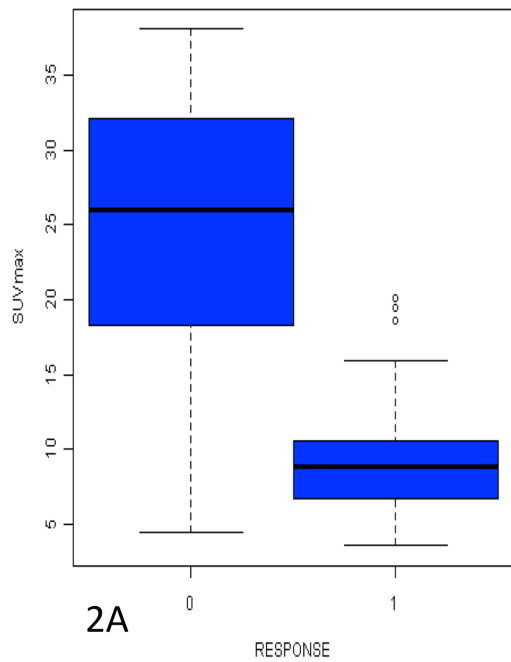


Figure 2. Figure 2A illustrates the difference in SUVmax values between non-responders (left boxplot) and responders (right box plot). Figure 2B shows the ROC curve analysis for SUVmax and SUVmean to separate responders from non-responders (AUC respectively 0.873 for SUV max and 0.819 for SUVmean).